Tuberculosis 96 (2016) 1–12

Contents lists available at ScienceDirect

Tuberculosis

journal homepage: http://intl.elsevierhealth.com/journals/tube

MODEL SYSTEMS

Ultra low dose aerosol challenge with *Mycobacterium tuberculosis* leads to divergent outcomes in rhesus and cynomolgus macaques

Sally Sharpe [a, *], Andrew White [a], Fergus Gleeson [b], Anthony McIntyre [b], Donna Smyth [a], Simon Clark [a], Charlotte Sarfas [a], Dominick Laddy [c], Emma Rayner [a], Graham Hall [a], Ann Williams [a], Mike Dennis [a]

[a] Public Health England, Porton Down, Wiltshire, UK
[b] The Churchill Hospital, Headington, Oxford, UK
[c] Aeras, Rockville, MD 20850, USA

ARTICLE INFO

Article history:
Received 19 August 2015
Received in revised form
2 October 2015
Accepted 6 October 2015

Keywords:
Tuberculosis
Non-human primate
Aerosol challenge
Low dose

SUMMARY

Well characterised animal models that can accurately predict efficacy are critical to the development of an improved TB vaccine. The use of high dose challenge for measurement of efficacy in Non-human primate models brings the risk that vaccines with the potential to be efficacious against natural challenge could appear ineffective and thus disregarded. Therefore, there is a need to develop a challenge regimen that is more relevant to natural human infection. This study has established that ultra-low dose infection of macaques via the aerosol route can be reproducibly achieved and provides the first description of the development of TB disease in both rhesus and cynomolgus macaques following exposure to estimated retained doses in the lung of less than 10 CFU of *Mycobacterium tuberculosis*. CT scanning *in vivo* and histopathology revealed differences in the progression and burden of disease between the two species. Rhesus macaques exhibited a more progressive disease and cynomolgus macaques showed a reduced disease burden. The ability to deliver reproducible ultra-low dose aerosols to macaques will enable the development of refined models of *M. tuberculosis* infection for evaluation of the efficacy of novel tuberculosis vaccines that offers increased clinical relevance and improved animal welfare.

1. Introduction

Tuberculosis (TB) is a major global health problem, with 9 million new cases and nearly 1.5 million deaths annually [1]. With a third of the world's population estimated to be infected, and the effects of TB infection compounded by the emergence of multi-drug resistant strains and HIV co-infection, there is an urgent need for improved interventions, including a vaccine. The only currently available vaccine is *Mycobacterium bovis* Bacille Calmette Guerin (BCG) which protects children from developing severe TB disease [2], but it is unsuitable for use in people whose immune system is compromised, and has mostly failed to protect against pulmonary TB in adults [3].

The lack of a defined immunological correlate of protection for TB means that, in order to assess efficacy, candidate TB vaccines must enter large clinical trials involving thousands of at-risk individuals in endemic countries [4]. Therefore, preclinical animal models that can accurately predict the effectiveness of vaccines in humans through challenge studies are critical to achieving the goal of an improved TB vaccine. Because of their close similarity to humans, non-human primates (NHP) are excellent potential models of tuberculosis [5–7]. Reviews of published studies using the TB NHP model [5–7] reveal that the selection of model parameters, including the macaque species and route and size of the challenge dose, can affect the outcome of experimental TB exposure in NHPs. Both rhesus [8–15] and cynomolgus macaque species [11,16–19] are used to evaluate the efficacy of new TB vaccine candidates. Both species recapitulate aspects of human TB but which provides the most appropriate model for vaccine evaluation is a subject of debate.

The quantity of *M ycobacterium tuberculosis* administered to evaluate vaccine efficacy is critical to the outcome of an efficacy study. The dose needs to be sufficient to induce a consistent and

* Corresponding author. Tel.: +44 (0) 1980 612811; fax: +44 (0) 1980. 611310.
E-mail address: sally.sharpe@phe.gov.uk (S. Sharpe).

http://dx.doi.org/10.1016/j.tube.2015.10.004

measureable disease burden in all exposed animals but not so large as to overwhelm any protection provided by the host response. The readouts used routinely to measure the efficacy of new TB vaccines in NHP models such as changes in clinical parameters, bacterial burden and qualitative gross pathology and histopathological scoring systems have limited sensitivity [20]. This has necessitated the use of high doses of TB for challenge, which far exceed the estimated doses encountered during natural exposure, and bring the risk that potentially useful vaccines could be disregarded. Consequently, there is a growing view that a lower challenge dose (less than 10 infectious bacilli) that more closely resembles natural infection is required to refine the vaccine assessment process. The physical properties of *M. tuberculosis* (e.g. clumping) create difficulties in generating inocula containing very few bacilli from high titre stocks but the process of aerosolisation disrupts bacterial aggregates and generates aerosol particles which mostly contain single bacteria. Measurement of the outcome of very low dose challenge requires improved tools to provide more sensitive readouts of disease burden such as those offered by advanced *in vivo* imaging [21–23].

With the ultimate aim to establish an NHP model for vaccine assessment based upon ultra-low dose infection the present study was set up to provide proof of concept for the reproducible delivery of an ultra-low dose (ULD) of *M. tuberculosis* to macaques by the aerosol route; to characterise the outcome of ULD aerosol exposure; and compare the resulting disease in the two macaque species. Furthermore the potential benefit of computed tomography (CT) to provide sensitive measures of disease burden that could be used as readouts for evaluation of vaccine efficacy following low dose challenge was investigated.

2. Materials and methods

2.1. Experimental animals

Eight male rhesus macaques and eight male cynomolgus macaques, aged 3–4 years, were obtained from established UK breeding colonies. Genetic analysis of these colonies has previously confirmed the rhesus macaques to be of the Indian genotype and cynomolgus macaques of Indonesian genotype. Absence of previous exposure to mycobacterial antigens was confirmed by a tuberculin skin test and screening using an *ex-vivo* IFN-γ ELISPOT (MabTech, Nacka. Sweden) to measure responses to PPD (SSI, Copenhagen, Denmark), and pooled 15-mer peptides of ESAT6 and CFP10 (Peptide Protein Research LTD, Fareham, U.K.).

Animals were housed in compatible social groups, in accordance with the Home Office (UK) Code of Practice for the Housing and Care of Animals Used in Scientific Procedures (1989), (now updated to Code of Practice for the housing and Care of Animals Bred, Supplied or Used for Scientific Purposes, December 2014, and the National Committee for Refinement, Reduction and Replacement (NC3Rs), Guidelines on Primate Accommodation, Care and Use, August 2006 (NC3Rs, 2006)). Animals were sedated by intramuscular (IM) injection with ketamine hydrochloride (Ketaset, 100 mg/ml, Fort Dodge Animal Health Ltd, Southampton, UK; 10 mg/kg) for procedures requiring removal from their housing. None of the animals had been used previously for experimental procedures. All animal procedures were approved by the Public Health England Ethical Review Committee, Porton Down, UK, and authorised under an appropriate UK Home Office project license.

2.2. Clinical procedures

Animals were monitored daily for behavioural and clinical changes. Behaviour was evaluated for contra-indicators including depression, withdrawal from the group, aggression, changes in feeding patterns, breathing pattern, respiration rate and cough. Prior to blood sample collection, aerosol challenge and euthanasia, animals were weighed, examined for gross abnormalities and body temperature measured. Red blood cell (RBC) haemoglobin levels were measured using a HaemaCue haemoglobinometer (Haemacue Ltd, Dronfield, UK) to identify the presence of anaemia, and erythrocyte sedimentation rates (ESR) were measured using the Sediplast system (Guest Medical, Edenbridge, UK) to detect and monitor inflammation induced by infection with *M. tuberculosis*.

2.3. M. tuberculosis challenge strain

The Erdman K01 stock (HPA-Sept 2011) used for challenge was prepared from stocks of the *M. tuberculosis* Erdman strain K 01 (BEI Resources). A stock suspension was initially prepared from a 5 ml bacterial starter culture originally generated from colonies grown on Middlebrook 7H11 supplemented with oleic acid, albumin, dextrose and catalase (OADC) selective agar (BioMerieux, UK). A liquid batch culture was then grown to logarithmic growth phase in 7H9 medium (Sigma–Aldrich, UK) supplemented with 0.05% (v/v) Tween 80 (Sigma–Aldrich, UK). Aliquots were stored at −80 °C. Titre of the stock suspension was determined from thawed aliquots by enumeration of colony forming units cultured onto Middlebrook 7H11 OADC selective agar.

2.4. Aerosol exposure

2.4.1. Apparatus and procedure

The methodology and apparatus used to deliver *M. tuberculosis* via the aerosol route was as previously described [14,20,24]. In brief, the aerosols were generated from a suspension of *M. tuberculosis* at a pre-determined concentration (see below) using a 3-jet Collison nebuliser (BGI) and delivered, using a modified Henderson apparatus [25] controlled by an AeroMP (Biaera) control unit [26], to the nares of each sedated animal via a modified veterinary anaesthesia mask. A 'head-out', plethysmography chamber (Buxco, Wilmington, North Carolina, USA) enabled the aerosol to be delivered simultaneously with the measurement of respiration rate.

2.4.2. Quantification of ultra-low aerosol dose

The number of bacilli deposited and retained in the lungs of macaques cannot be measured directly and the quantification of the dose must be calculated from the concentration of viable organisms in the aerosol (C_{aero}) and the volume of aerosol inhaled by the animal. This 'presented dose' (PD) is the number of organisms which the animals inhale. C_{aero} is either measured directly using air sampling within the system or may be calculated using the concentration of organisms in the nebuliser (C_{neb}) and a 'spray factor' which is a constant derived from data generated for the specific organism with identical aerosol exposure parameters. The calculations to derive the PD and the retained dose (the number of organisms assumed to be retained in the lung) have been described previously for high/medium aerosol doses [20,24]. Direct measurement of C_{aero} would not be possible for an ultra-low dose challenge and therefore the dose calculations were based upon C_{neb} and the spray factor. Aerosol challenge data from previous experiments were used to develop and verify the calculation which would predict the retained dose, and a nebuliser concentration was selected to result in a retained dose of approximately 5 viable bacilli.

2.4.3. Macaque aerosol exposure

Four rhesus and four cynomolgus macaques (group A) were exposed to aerosols of *M. tuberculosis* five weeks before the second

group of four rhesus and four cynomolgus macaques (group B) (Figure 1). The study was conducted in two phases to allow evaluation of the reproducibility of the aerosol delivery system.

2.5. Computed tomography (CT) imaging

CT scans were collected from animals using a 16 slice Lightspeed CT scanner (General Electric Healthcare, Milwaukee, WI, USA), three, eight and eleven weeks after aerosol exposure to *M. tuberculosis* (Figure 1) as described previously [27,28]. In order to enhance visualisation of lesions and lymph nodes, Niopam 300 (Bracco, Milan, Italy), a non-ionic, iodinated contrast medium, was administered intravenously (IV) at 2 ml/kg body weight. Scans were evaluated for the number and distribution of pulmonary lesions across lung lobes and the presence of nodule cavitation, conglomeration, consolidation as an indicator of alveolar pneumonia and a 'Tree-in–bud' pattern as an indicator of bronchocentric pneumonia. The lung-associated lymph nodes were assessed for enlargement and the presence of necrosis.

2.6. Immune response analysis: Interferon-gamma (IFN-γ) ELISpot

The *M. tuberculosis*-specific immune response was evaluated at two weekly intervals throughout the study (Figure 1). Peripheral blood mononuclear cells were isolated from heparin anti-coagulated blood using standard methods. An IFN-γ ELISpot assay was used to estimate the numbers and IFN-γ production capacity of mycobacteria-specific T cells in PBMCs using a human/simian IFN-γ kit (MabTech, Nacka. Sweden), as described previously [29].

2.7. Necropsy

The necropsies were conducted either, four weeks (Group A) or 12 weeks (Group B) after aerosol exposure to *M. tuberculosis* (Figure 1). Animals were anaesthetised and clinical data collected. Blood samples were taken prior to euthanasia by intra-cardiac injection of a lethal dose of anaesthetic (Dolelethal, Vétoquinol UK Ltd, 140 mg/kg). A post-mortem examination was performed immediately and gross pathological changes were scored using an established system based on the number and extent of lesions present in the lungs, spleen, liver, kidney and lymph nodes, as described previously [20]. Samples of spleen, liver, kidneys and tracheobronchial, inguinal and axillary lymph nodes were removed and sampled for quantitative bacteriology. The lung, together with the heart and attached tracheobronchial and associated lymph nodes, were removed intact. The lymph nodes were measured and examined for lesions. These were fixed by intra-tracheal infusion with 10% neutral buffered formalin (NBF) using a syringe and 13CH Nelaton catheter (J.A.K. Marketing, York, UK). The catheter tip was inserted into each bronchus in turn via the trachea; the lungs were infused until they were expanded to a size considered to be normal inspiratory dimensions, and the trachea ligated to retain the fluid. The infused lung was immersed in 10% NBF. In addition, samples of kidneys, liver, spleen, and sub clavicular, hepatic inguinal and axillary lymph nodes were fixed in 10% NBF.

2.8. Thoracic lymph node evaluation

At necropsy, eight thoracic lymph nodes (right and left cranial, carinal, sub-clavicular, para-tracheal) were measured and scored

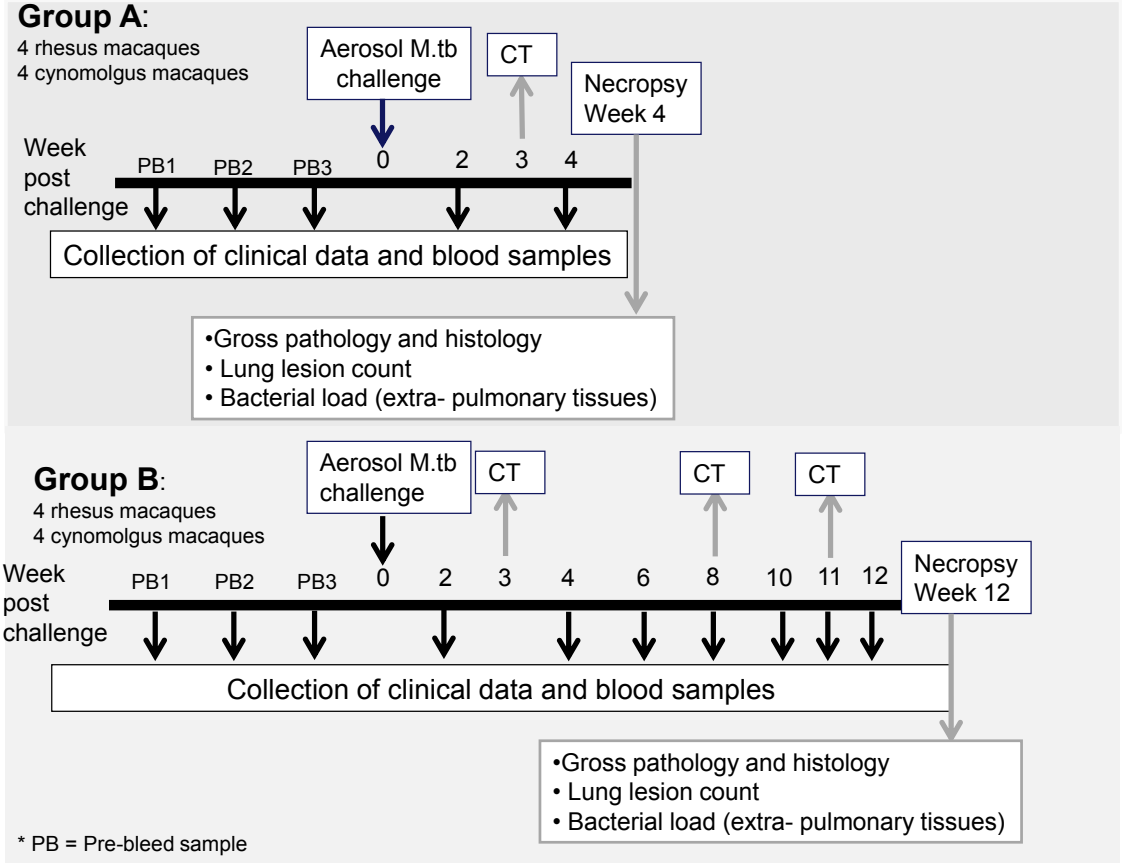

Figure 1. Experimental study design.

for enlargement according to the system in Table 1A. Nodes measuring 5 mm or more were considered to be enlarged. The enlargement scores attributed to each individual node were summed to provide a total score for the animal (maximum score = 24). In addition, the proportion of thoracic lymph nodes showing enlargement in each animal was calculated: number of lymph nodes measuring >5mm/8, where 8 = the number of lymph nodes evaluated.

2.9. Pathology studies

2.9.1. Gross examination following fixation

The fixed lungs were sliced serially and lesions counted as described previously [27]. Each lung lobe was evaluated separately and discrete lesions were counted in the parenchyma. Where lesions had coalesced, these were measured and recorded. Lung-associated lymph nodes, particularly around the tracheal bifurcation, were dissected and weighed. The remaining tissues were examined during trimming.

2.9.2. Histopathological examination

A representative samples from each lung lobe (seven per animal) and other organs, were processed to paraffin wax, sectioned at 3–5 μm and stained with haematoxylin and eosin (HE). For each lung lobe, tissue slices containing obvious lesions were chosen for histological examination. Where gross lesions were not visible, a sample was taken from a pre-defined anatomical location from each lobe to establish consistency between animals. Sections of lung-associated lymph nodes (trachea-bronchial at the bifurcation and cranial and caudial to the bifurcation) and other tissues were evaluated for the presence of tuberculous lesions. Lesions in the lung parenchyma were identified, categorised and counted as described previously [27]. Briefly, lesions defined as “unorganised” (Types 1–3) were those lacking a peripheral cuff of lymphocytes, while “organised” lesions were those with a cuff of lymphocytes (Types 4 and 5). In one HE stained section from each lung lobe, granulomas types, as described in Table 1B, were counted and recorded. Furthermore, additional, morphological features were recorded: airway invasion, lymphatic inflammation/involvement, arterial wall infiltration by inflammatory cells and granulomas in bronchovascular, connective tissue. To evaluate the degree of necrosis in tracheobronchial lymph nodes, an HE stained section of an enlarged node from each animal, was scanned digitally (3D Histotech Panoramic 250) using “Panoramic Viewer software” Version 1.15.2 SP 2 (3D Histotech Ltd, Budapest). The necrotic areas within the scanned sections were defined and the resulting surface area divided by the total surface area of the lymph node, then multiplied by 100 to give a percentage.

Table 1
Pathology scoring systems.

A. Thoracic lymph node enlargement score	
Size (mm)	Enlargement score
<5	0
5–10	1
>10–20	2
>20	3

B. Lung parenchyma lesion categorisation system	
Lesion type	Lesion characteristics
1	Small, diffuse foci of macrophages and lymphocytes with scattered neutrophils and eosinophils lacking clearly defined boundaries
2	Larger unorganised lesions composed of similar inflammatory cells to type 1 lesions, circumscribed foci forming a more defined, frequently circular granuloma with variably demarcated borders.
3	Granulomas, characterised by nuclear pyknosis and karyorrhexis with the loss of cellular architecture and the presence of focal necrosis.
4	Granulomas show evidence of organisation of lymphocytes to a peripheral location
5	Granulomas show central necrosis

2.10. Bacteriology

The spleen, kidneys, liver and tracheobronchial lymph nodes were sampled for the presence of viable *M. tuberculosis* post-mortem as described previously [14]. Weighed tissue samples were homogenised in 2 ml of sterile water, then either serially diluted in sterile water prior to being plated, or plated directly onto Middlebrook 7H11 OADC selective agar. Plates were incubated for 3 weeks at 37 °C and resultant colonies were confirmed as *M. tuberculosis* and counted.

2.11. Statistical analyses

Comparison of *ex-vivo* ELISpot assay responses was completed using the area under the curve (AUC) of each animal's response calculated using Sigmaplot version 10 (Systat Software Inc, Hounslow, UK). AUC values were compared between test groups using the non-parametric Mann–Whitney U test, Minitab version 15 (Minitab Ltd, Coventry, UK). Differences in the qualitative pathology scores were compared between species and test groups using the non-parametric Mann–Whitney U test, Minitab version 15 (Minitab Ltd, Coventry, UK). The Spearman correlation test was used to determine the level of correlation between study parameters using GraphPad Prism, version 5.01 (GraphPad Software Inc, La Jolla, California, USA).

3. Results

3.1. Reproducible aerosol delivery of ultra-low doses of *M. tuberculosis*

Exposure to ULD aerosols of *M. tuberculosis* resulted in an established infection in all challenged animals. The presented and estimated retained aerosol doses (Table 2) were consistent across the rhesus and cynomolgus macaque species and between study groups A and B which received aerosol challenge five weeks apart. Whether grouped by species or study group, the average presented dose was calculated as 24 or 25 cfu and the estimated retained dose in the lung was 3 or 4 cfu.

The inoculum delivered by aerosol was also quantified as lesion forming units (LFU) defined as the number of TB-induced nodules counted from CT scans collected 3 weeks after aerosol exposure, and was assumed to provide a measure of primary lesions. The number of TB-induced nodules counted from CT scans collected three weeks after aerosol exposure (LFU) was similarly low and consistent across species (range: 1 to 10) with a median of six nodules for all animals in the study and medians of six nodules for rhesus and four nodules in cynomolgus macaques. The number of LFU counted in animals in group A were not significantly different to the number counted in animals in group B for either species (rhesus macaque, $p=0.2857$; cynomolgus macaque, $p = 0.0857$).

3.2. Clinical assessment post exposure

All macaques controlled disease after ULD aerosol challenge. None of the animals of either species exhibited abnormal

Table 2
Aerosol challenge doses of *M. tuberculosis* delivered to rhesus and cynomolgus macaques.

Exposure group	Species	Animal identification number	Presented dose (cfu)	Estimated retained dose (cfu)	Lesion forming units 3 weeks post-aerosol exposure
Group A	Rhesus	T7	24	3	6
		T21	24	3	10
		T26	25	4	6
		T41	25	4	9
	Cynomolgus	980BEEA	25	4	7
		978AJB	23	3	7
		970CIA	27	4	4
		545ACEA	25	4	8
Group B	Rhesus	T51	21	3	1
		T59	25	4	3
		T64	24	3	6
		T75	24	3	9
	Cynomolgus	044HAFC	23	3	2
		031 MN	28	4	1
		406ADM	24	3	4
		980ABAGB	23	3	4
		406ADM	24	3	4
		980ABAGB	23	3	4

behaviour, signs of respiratory disease or coughing. However both rhesus and cynomolgus macaques had minor losses in body weight (<4% peak post exposure weight) over the first 4 weeks after aerosol exposure. A trend for more, but non-significant (<10% peak post challenge weight) weight loss was seen in rhesus macaques at week 12, with three animals showing losses of between 2 and 8%; by contrast, weight losses of <2% were seen in the cynomolgus macaques. Body temperature, red blood cell haemoglobin concentrations and levels of inflammatory markers (ESR) remained within normal range throughout the study period.

3.3. CT evaluation of pulmonary disease

Assessment of the number and distribution of TB-induced nodules in the lungs from the CT scans at 3, 8 and 11 weeks after aerosol exposure to *M. tuberculosis* showed an increase in nodule numbers over time, which tended to be greater in rhesus macaques. Aerosol delivery led to the development of nodules in multiple lung lobes by week 3; lesions were more prevalent in the right lung lobes (14 of the 16 macaques in the study) than in the left lung lobes (8 of 16 macaques in the study), and distribution was similar between the species (Figure 2). Nodules were detected in previously unaffected lung lobes in the cynomolgus and in the rhesus macaques by eight and eleven weeks, respectively. Nodule cavitation was observed in rhesus macaques from week 8 (Table 3, supplementary Tables 1a and 1b), but not in cynomolgus macaques. Features of pneumonia (consolidation and a "tree-in–bud" pattern) were detected at similar frequencies in both species at weeks 3 and 8. Pneumonia was detected in three rhesus macaques at week 8 and persisted through to week 11, whereas it was detected in three cynomolgus macaques but persisted to week 11 in only one animal (Table 3, supplementary Tables 1a and 1b).

The frequency of necrotic lymph nodes associated with the lungs was similar between the macaque species, although a higher frequency of enlarged lymph nodes was seen in the rhesus macaques. Bronchial compression due to enlarged nodes was noted in one animal of each species at week eight.

3.4. IFNγ response to infection

An *ex-vivo* ELISPOT assay was applied at two weekly intervals throughout the study to evaluate the *M. tuberculosis*-specific immune response to infection. Response kinetics were similar in the two macaque species with peak responses detected six weeks after infection. However, the frequency of IFNγ secreting cells specific for TB antigens detected in rhesus macaques was higher than the frequencies seen in cynomolgus macaques (Figure 3). AUC analysis confirmed the difference in the PPD-specific response between the species to approach significance in the first four week period ($p = 0.05$) and for the response to be significantly higher in rhesus macaques during the 12 weeks ($p = 0.03$) after aerosol exposure. Responses to CFP10 and ESAT6 were not significantly different between the species during the first four weeks after infection. However, by 12 weeks, responses to ESAT6 in rhesus macaques were significantly higher than the responses in the cynomolgus macaques ($p = 0.03$).

When all animals in the study were evaluated as a single group, a significant correlation was found between the number of pulmonary nodules identified on CT scans three weeks after aerosol exposure and the AUC of the PPD-specific response measured during the first four weeks after infection ($p = 0.01$, $r = 0.61$), and a correlation that approached significance was seen with the response to ESAT6 ($p = 0.06$, $r = 0.548$). The number of nodules counted on the eight week CT scans positively correlated with the AUC of the responses made in the eight week period after exposure, although only the correlation with the CFP10-specific response reached significance ($p = 0.0315$, $r=0.7807$). Correlations that reached significance were not seen between the AUC of the PPD, CFP10 or ESAT6 -specific responses measured during the first 12 weeks after infection in all study animals and the number of nodules counted from the CT scans collected at week 12 (PPD, $p = 0.08$, $r = 0.67$; ESAT6, $p = 0.097$, $r = 0.6386$; CFP10, $p = 0.152$, $r = 0.5663$).

When relationships were evaluated in the rhesus and cynomolgus species separately correlations between the AUC of the responses measured in the four, eight or 12 week periods after exposure, and nodule numbers from the CT scans at weeks three or 11 after exposure, did not reach significance.

3.5. Pathological evaluation of disease burden

Disease burden was evaluated four weeks after aerosol exposure in four rhesus and four cynomolgus macaques, and 12 weeks after exposure in the remaining eight animals. The gross pathology score system did not reveal significant differences between the level of

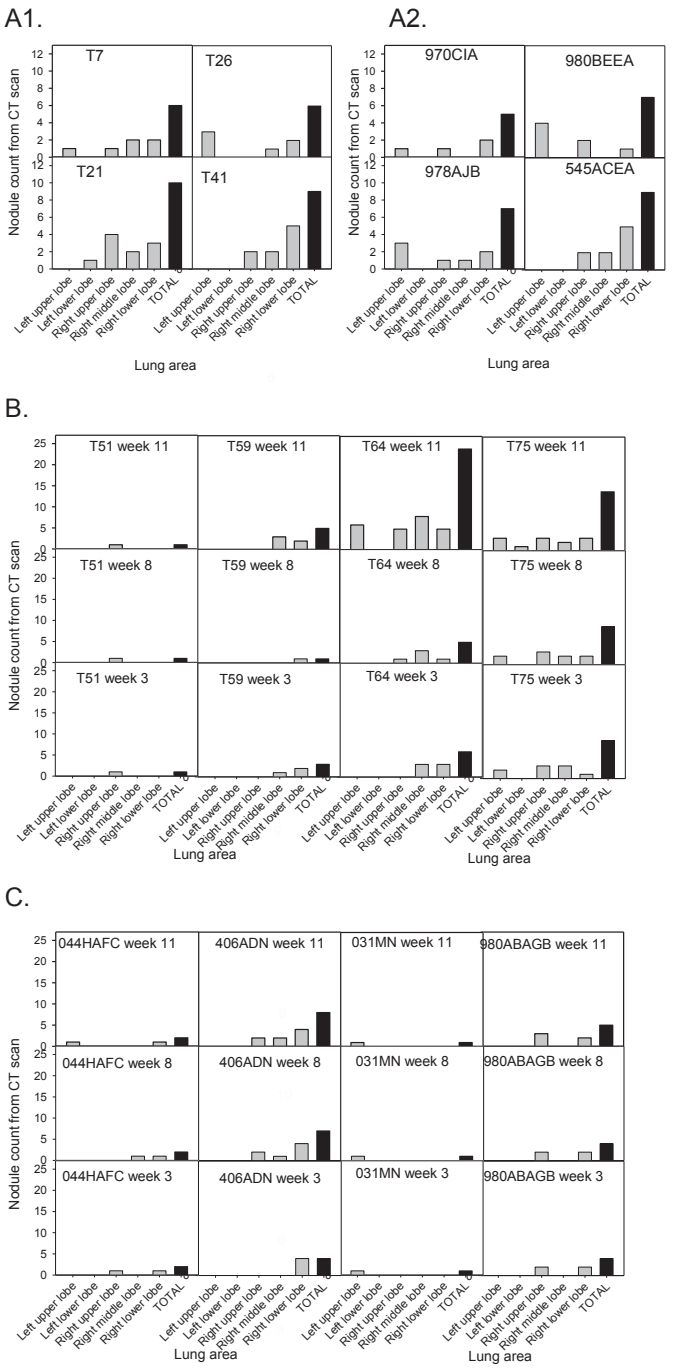

Figure 2. Number of TB-induced nodules counted from the CT scans collected from rhesus (panel A1) and cynomolgus macaques (panel A2) in Group A (4 week study), and rhesus (panel B) and cynomolus macaques (panel C) in group B (12 week study). Grey fills shows the number of lesions in each lung lobe and black fills show the total number of nodules in the lung.

disease present in rhesus and cynomolgus macaques at either four *($p = 0.47$)* or 12 weeks *($p = 0.06$)* after TB exposure (Figure 4A). However, there was a trend for scores to increase over time in both species and the difference seen at week 12 approached significance.

Gross lesion data following fixation and sectioning of the lung lobes are summarised in Table 4, and supplementary table 2. In rhesus macaques the mean number of discrete (10.8 ± 7.8 to 14 ± 22.5) and coalesced (3.8 ± 0.8 to 4.3 ± 2.9) lesions noted increased between four and 12 weeks post challenge and

Table 3
Development of TB induced disease features identified using computed tomography in rhesus and cynomolgus macaques following exposure to ULD aerosols.

	Number of macaques showing TB feature/number in group															
	Week 3					Week 8					Week 11					
	Lung nodules		Pneumonia		Lung associated lymph nodes	Lung nodules		Pneumonia		Lung associated lymph nodes	Lung nodules		Pneumonia		Lung associated lymph nodes	
	Conglomeration	Cavitation	Consolidation	Tree-in-Bud	Necrosis Enlarged	Conglomeration	Cavitation	Consolidation	Tree-in-Bud	Necrosis Enlarged	Conglomeration	Cavitation	Consolidation	Tree-in-Bud	Necrosis	Enlarged
Rhesus	0/8	0/8	1/8	1/8	0/8	2/4	2/4	3/4	2/4	3/4	1/4	3/4	3/4	2/4	3/4	0/4
Cynomolgus	0/8	0/8	1/8	0/8	0/8	1/4	0/4	3/4	1/4	2/4	0/4	0/4	1/4	1/4	3/4	1/4

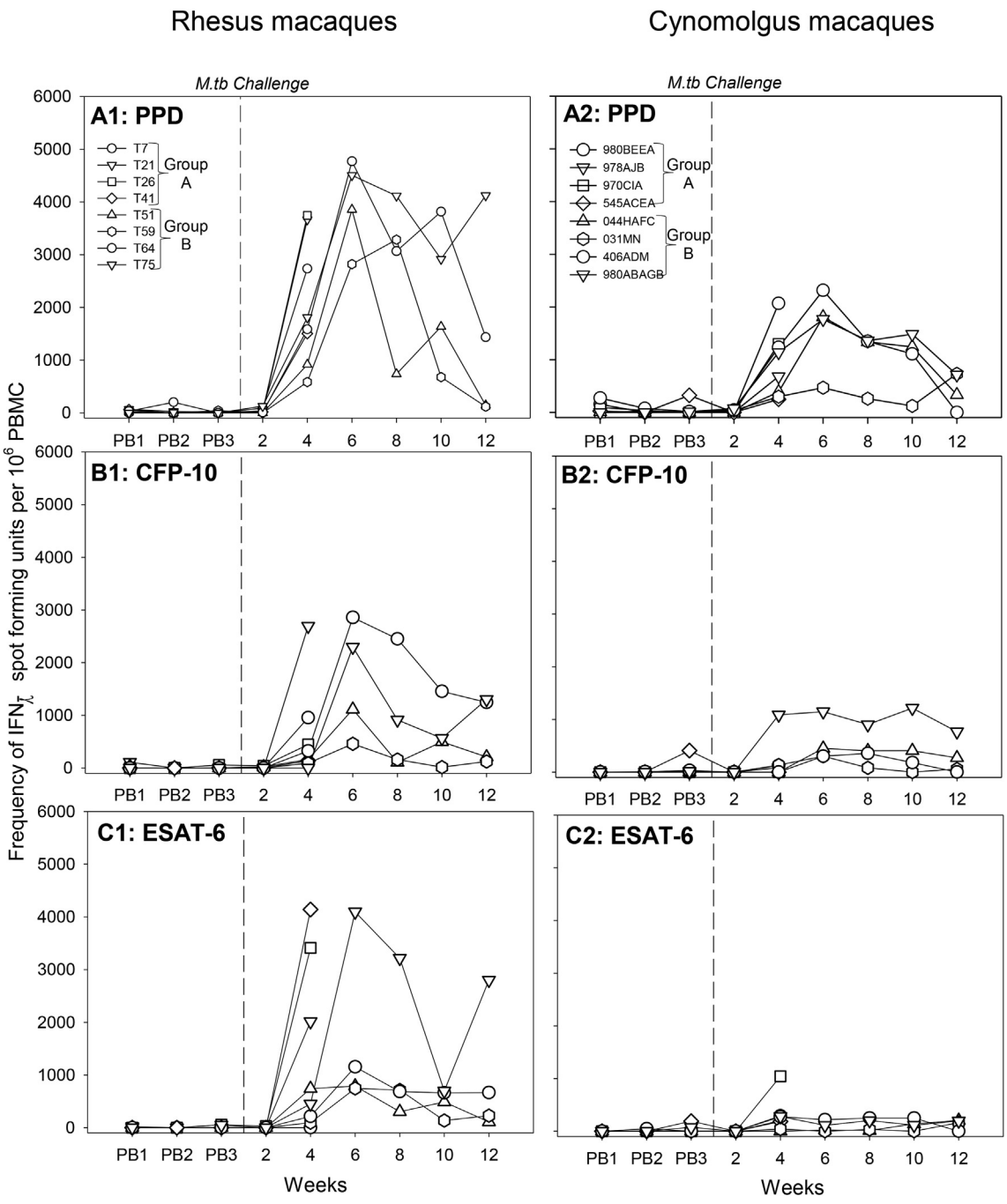

Figure 3. The frequency of *M. tuberculosis*-specific IFNγ secreting cells measured by *ex-vivo* ELISpot following exposure to ultra-low dose TB aerosols in peripheral blood mononuclear cells collected from rhesus macaques is shown in the panel on the left, and the panel on the right shows the frequencies in peripheral blood mononuclear cells collected from cynomolgus macaques. Plots A1 and A2 show the profiles of PPD-specific IFNγ secreting cells, Plots B1 and B2 show the profiles of CFP10-specific IFNγ secreting cells, and Plots C1 and C2 show the profiles of ESAT6-specific IFNγ secreting cells. Aerosol exposure to *M. tuberculosis* at week 0 is indicated by the dotted line. PB1, 2, 3 indicate responses determined on three occasions prior to exposure.

the mean volume of coalesced lesions increased from 9682 ± 4602 mm^3 to 20,092 ± 21,293 mm^3. By contrast, in the cynomolgus macaques, the mean number of discrete lesions decreased (19.3 ± 13.2 to 10.3 ± 7.2) between four and 12 weeks post challenge. At four and 12 weeks post challenge, only three coalesced lesions were observed at each time point; however, the mean gross volume increased from 447 ± 539 mm^3 to 1409 ± 1307 mm^3.

Enlarged tracheo-bronchial and associated lymph nodes were seen in both macaque species at four and 12 weeks after exposure to ULD TB aerosols. Application of a qualitative scoring system to evaluate the level of enlargement during gross examination revealed non-significant trends for the enlargement to be greater in rhesus than in cynomolgus at both four and 12 weeks post-challenge, and to increase over time in both species (Figure 4B). The proportion of tracheo-bronchial lymph nodes showing enlargement was greater in rhesus than in cynomolgus at both

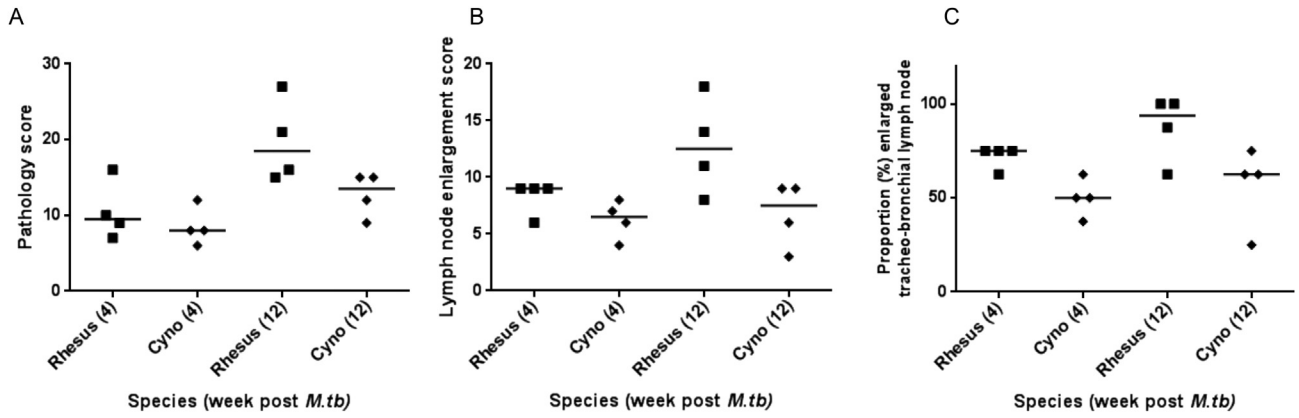

Figure 4. Disease burden measured four or twelve weeks after ultra-low dose aerosol exposure determined using a qualitative gross pathology scoring system applied at necropsy (plot A), tracheo-bronchial lymph node enlargement score (plot B) and the proportion of tracheo-bronchial lymph nodes showing enlargement (plot C) 4 and 12 weeks after exposure to ultra-low dose TB aerosols.

Table 4
Histopathological evaluation of the lungs and tracheobronchial lymph nodes: Summary of findings.

Group mean (range)								
Species	No. of pulmonary lesions				Coalesced volume of pulmonary lesions (mm^3)		Lymph node necrosis (%)	
	Discrete		Coalesced					
	Week 4	Week 12	Week 4	Week 12	Week 4	Week 12	Week 4	Week 12
Rhesus	10.8 (3–23)	14 (0–53)	3.8 (3–5)	4.3 (1–8)	9682 (4840–17040)	20,092 (3510–56,677)	40.4 (13.9–65.1)	57.3 (43.6–68.7)
Cynomolgus	19.8 (8–42)	10.3 (2–21)	0.8 (0–2)	0.8 (0–1)	447 (0–1320)	1409 (0–3549)	37.6 (26.3–56.3)	29.5 (0.2–46.8)

weeks four ($p = 0.0360$) and 12 ($p = 0.102$), and over time more tracheo-bronchial lymph nodes became enlarged in both species but differences did not reach significance (Figure 4C). Following fixation, the combined weights of the three heaviest, tracheo-bronchial lymph nodes in the rhesus macaques were 18.0 g and 20.8 g at four and 12 weeks post challenge, respectively. In cynomolgus macaques, the values were 10.6 g and 9.4 g, respectively.

Microscopic findings are illustrated in Figure 5. TB lesions were present in the lungs of all animals at four and twelve weeks post−challenge. In general, all lesion types were observed in the majority of animals at both time points, with Type 5 lesions being most frequent. In the cynomolgus macaques at four weeks post challenge, lesions were infrequent and often well demarcated (Figure 5A). By contrast, in rhesus macaques at the same time point, large, irregular areas of coalesced lesions with poorly demarcated borders were often noted (Figure 5B) as well as discrete lesion types. By 12 weeks post challenge, in the cynomolgus macaques, lesion size had generally decreased compared to the early time point (Figure 5C), although some coalesced lesions were still noted. However, in the rhesus macaques, large, coalescing areas were more prominent than at four weeks post challenge (Figure 5D), with scattered, discrete lesions also present. Small, cavitatory lesions (Figure 5D) were noted infrequently involving the airways in two animals. Additional, microscopic features, comprising airway invasion (Figure 5B, D, E), lymphatic involvement/inflammation (Figure 5E), vascular wall invasion by inflammatory cells (Figure F), and the presence of granulomas in broncho-vascular connective tissue (Figure 5E and F), were present at both four and 12 weeks post challenge in the lungs of rhesus macaques, but with reduced frequency at the latter time point. In the cynomolgus macaques, these features were also observed at four weeks post challenge; however, by 12 weeks, evidence of airway invasion was absent and lymphatic involvement/inflammation and the presence of granulomas in broncho-vascular connective tissue was reduced. There was no difference in the frequency of vascular invasion by inflammatory cells between the species.

The tracheobronchial lymph nodes examined from all animals at both time points were enlarged, with marked effacement of normal, nodal architecture by granulomatous inflammatory cells and prominent, caseous necrosis. The percentage of the lymph node surface area showing necrosis increased with time in both species (Table 4, supplementary Table 2), and was higher in the rhesus macaques compared to the cynomolgus macaques, although these differences did not reach statistical significance.

The prevalence of disease in extra-pulmonary tissues was similar between the species. In the rhesus macaques four weeks post challenge, tuberculous lesions were noted in the spleen (two out of four), liver (three out of four) and subclavicular lymph node (three out of four). At 12 weeks, lesions were noted in the spleen (one out of four), liver (four out of four), kidneys (two out of four), subclavicular lymph node (two out of four) and parietal pleura (two out of two examined). In the cynomolgus macaques at four weeks post challenge, extra-pulmonary lesions were observed in the spleen (three out of four), liver (three out of four), subclavicular lymph node (two out of four), right axillary lymph node (two out of four) and hepatic lymph node (two out of two examined). At 12 weeks post challenge, lesions were seen in the spleen (two out of four), liver (one out of four) and subclavicular lymph node (one out of three examined). All other tissues examined were negative for the presence of tuberculous lesions.

3.6. *Extra-pulmonary organ-specific bacterial burden*

The level of bacterial burden was evaluated in the liver, spleen, kidneys and tracheobronchial lymph nodes in all animals. A similar frequency of isolation from tissues and level of bacterial burden was seen across the species at week four and twelve together with a trend for less frequent isolation from tissues collected from animals

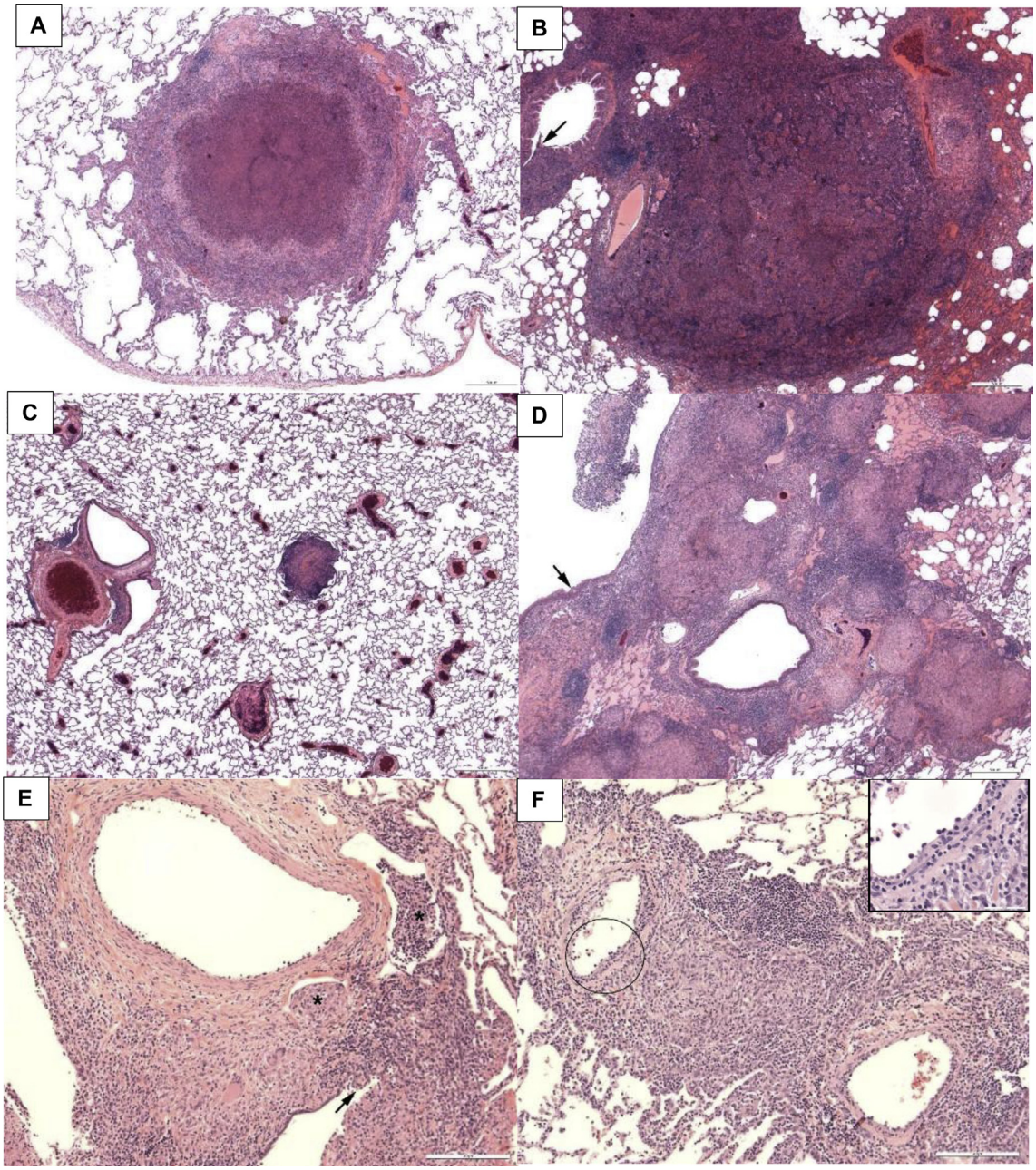

Figure 5. Examples of microscopic changes in the lung. (A) Animal 980BEEA (cynomolgus macaque, 4 weeks pc). Type 5 lesion with central necrosis; well demarcated from surrounding parenchyma. Calibration bar = 500 μm. HE. (B) Animal T7, (rhesus macaque, 4 weeks pc). Large, coalescing area of granulomatous inflammation with airway invasion (arrow). Calibration bar = 500 μm HE. (C) Animal 044HAFC (cynomolgus macaque, 12 weeks post challenge). Small, well demarcated, Type 5 lesion. Calibration bar = 500 μm. HE. (D) Animal T64 (rhesus macaque, 12 weeks post challenge). Irregular, large area of coalescing, granulomatous inflammation with airway invasion (arrow). Calibration bar = 500 μm. HE. (E) Animal 980BEEA (cynomolgus macaque, 4 weeks post challenge). Broncho-vascular, granulomatous inflammation with lymphatic involvement (asterisks) and airway invasion (arrow). Calibration bar = 200 μm HE. (F) Animal T75 (rhesus macaque, 12 weeks post challenge). Granulomatous inflammation in broncho-vascular connective tissue, surrounding and infiltrating arteries. Calibration bar = 200 μm. Inset, arterial wall infiltration by inflammatory cells. Calibration bar = 50 μm HE.

at week twelve than week four in both species (Table 5). *M. tuberculosis* was most commonly isolated from the tracheobronchial lymph nodes, which showed the highest cfu/g burden of the tissues assessed.

4. Discussion

Well characterised animal models that can accurately predict the effectiveness of vaccines are critical to achieving the goal of an improved TB vaccine. There is a consensus that the challenge dose used to evaluate vaccine efficacy should be a balance between a dose sufficiently low to simulate natural human exposure to *M. tuberculosis* whilst retaining the ability to reliably infect all of the challenged animals. This study has established that ultra-low dose infection of macaques via the aerosol route can be reproducibly achieved. Following exposure to aerosols containing <28 cfu *M. tuberculosis* Erdman, animals were estimated to have retained a dose of three or four bacilli in the lungs. These estimates are supported by the findings from CT scans taken three weeks after exposure, that show a median number of six TB-induced nodules in the lungs of each animal in the group. As the aerosolisation process creates mono-dispersed particles, it can be assumed that TB bacilli

Table 5
Frequency of isolation of *M. tuberculosis* from tissues.

Species	Week pc	No. per group Mtb isolated (N = 4)					
		Spleen	Kidney	Liver	Tracheobronchial LN	Blood	Urine
Rhesus	4	4	4	2	4	0	0
Cynomolgus	4	4	3	3	4	0	1
Rhesus	12	2	3	2	4	0	0
Cynomolgus	12	3	2	2	3	0	1

are delivered individually to the lung; thus, the number of nodules seen three weeks after exposure reflects the retained dose, as each nodule is highly likely to have been initiated by a single bacillus [30]. Lesions were identified more frequently in the right lung lobes than the left lobes, and this may be a characteristic of the bronchial anatomy in macaques leading to preferential distribution of the low presented dose. The aerosol dose was highly reproducible within and between the macaque species, and between replicate aerosol challenges separated by five weeks, demonstrating the high degree of control over experimental parameters offered by aerosol infection using our aerosol infection protocols.

The dose delivered in this study was lower than any of those used in previously reported studies of experimental aerosol TB infection. Studies in rhesus macaques conducted between 1966 and 1975 described the use of aerosol doses of *M. tuberculosis* between 11 and 50 cfu [8–10,31], and studies reported from 2002 have used larger aerosol doses of up to 500 cfu [14,20,32,34]. The only report of *M. tuberculosis* aerosol exposure to cynomolgus macaques used doses in excess of 30 cfu [20]. The inoculum size used in the present study is also lower than those reported in macaque studies in which *M. tuberculosis* was delivered either by intra-tracheal installation or intra-bronchial placement, where typically low dose models use 25 cfu [19,30,33,35–38] and higher dose models typically use inoculum sizes ranging between 50 and 3000 cfu [11,13,19,21,39–41]. Therefore, this is the first description of the development of TB disease in both rhesus and cynomolgus macaques following exposure to doses of less than 10 cfu of *M. tuberculosis* and provides the first opportunity to directly compare the outcome of a very low dose infection between the two macaque species.

Sequential images collected using CT scanning *in vivo* revealed the development of progressive disease in the rhesus macaques whereas, the disease in cynomolgus macaques generally appeared to be more controlled, even 12 weeks after challenge. Similarly, results of analyses applied *post mortem* were indicative of a higher level of pulmonary disease in the rhesus macaques than in the cynomolgus macaques at both four and 12 weeks after challenge. The rhesus possessed higher numbers of lesions, coalesced lesions of greater volume, an increased frequency of microscopic disease features, and a higher level of tracheobronchial lymph node involvement, with nodes showing more enlargement and necrosis. The discrete and coalesced lesions in both species were of similar appearance and generally reflected those described previously [22,27,42], suggesting that the disease initiated following exposure to very low dose aerosols resembles that initiated following exposure to larger doses of *M. tuberculosis*. The difference in the disease burden induced following infection between the species primarily correlates with that described in previous studies reporting that after inoculation with larger numbers of cfu, where cynomolgus macaques are generally considered to be relatively resistant to tuberculosis and will develop active, chronic or latent TB [11,33,35] depending on strain, dose and route. In contrast, rhesus macaques appear to be more susceptible [11,20] and progressive disease has been reported to develop after low dose challenge [9,38,43]. The small groups sizes used and the short duration of the study reported here may have limited the ability to demonstrate statistically significant differences between the species, and this time course was not designed to evaluate whether the immune response of the macaques in this study could have gained sufficient control over the disease to result in latency. Understanding the differences in outcome of TB infection in rhesus and cynomolgus macaques is essential for future study design and refinement enabling the selection of the most appropriate species to address the study aims.

The number of TB bacilli encountered during challenge by the macaques in this study is more akin to the levels encountered during natural transmission than those used in high dose challenge systems [13,14,42]. Whilst this potentially provides a more realistic test for efficacy afforded by new vaccines, the ability to demonstrate efficacy within a model is dependent on the sensitivity and relevance of the readouts used to discriminate between vaccinated and unvaccinated test groups. Following infection initiated with larger numbers of bacilli, marked changes in clinical parameters occur as the disease progresses, such as, loss of body weight, elevation of body temperature and levels of inflammatory markers [11,13,14,33,35], and in this situation, clinical measures provide a valuable readout of vaccine efficacy. However, the macaques in this study did not exhibit abnormal behaviours or marked clinical signs when infection was initiated with very low numbers of bacilli. Therefore, in very low dose models, changes in clinical parameters may not be sufficiently discriminatory meaning that alternative, more sensitive approaches to evaluate disease burden are required.

Computed tomography allowed the identification of changes *in vivo* that provided the only clinical measure that was able to identify differences in disease development between the macaque species during this study, and thus provided a critical tool for evaluation of disease burden during the course of an experimental infection. The correlation seen in this study between pulmonary burden measured as number of nodules on CT scans, and the early IFNγ immune response, supports the hypothesis that the initial response to challenge, as measured by ELISPOT, reflects the antigen load. Whilst computed tomography undoubtedly provides a sensitive measure of disease development, further work is required to determine whether the readout used in this study would be sufficient to provide a measure of vaccine efficacy, or whether the additional metabolic activity measures provided by PET-CT will be required [23]. The frequency of *M. tuberculosis* antigen-specific IFNγ-secreting cells measured by ELISPOT in the rhesus macaques in this study were at similar levels to those measured after high dose challenge [14] and further supports the use of the ULD model for the study of potential immune correlates and biomarkers.

This study has established proof of concept for the reproducible delivery of very low dose aerosols of *M. tuberculosis* to rhesus and cynomolgus macaques and described differences in disease outcome between the species. This will enable the development of a more refined model of *M. tuberculosis* infection that will be a valuable addition to the portfolio of models already in use to evaluate the efficacy of novel tuberculosis vaccines and therapeutics. Such a model would have advantages over high dose challenge

models not only due to its increased relevance to human infection, but also with regard to the improvement in the welfare of animals used in the efficacy studies through reduction of the disease burden.

Acknowledgements

This work was supported by Aeras and the Department of Health, UK. The views expressed in this publication are those of the authors and not necessarily those of the Department of Health. We thank the staff of the Biological Investigations Group at PHE Porton and the PHE macaque colonies for assistance in conducting studies; Tracy Benford and Faye Lanni for bacteriology and aerobiology support, Katie West for support with the immune response analysis, Professor Geoff Pearson for histopathology peer review and Laura Hunter for histology support and Aeras NHP Model Development Group for constructive discussions.

Funding: None.

Competing interests: None declared.

Ethical approval: All procedures described in this paper were conducted under the authority of a Home Office approved project licence that had undergone ethical review by the Institute's Animal Welfare and Ethical Review Body as required under the UK Animals (Scientific Procedure) Act, 1986.

Appendix A. Supplementary data

Supplementary data related to this article can be found at http://dx.doi.org/10.1016/j.tube.2015.10.004.

References

[1] Zumla A, George A, Sharma V, Herbert RHN, of Ilton Baroness Masham, Oxley A, Oliver M. The WHO 2014 global tuberculosis report–further to go. Lancet Glob Health 2015;3:e10–2.
[2] Trunz BB, Fine P, Dye C. Effect of BCG vaccination on childhood tuberculous meningitis and miliary tuberculosis worldwide: a meta-analysis and assessment of cost-effectiveness. Lancet 2006;367:1173–80.
[3] Colditz GA, Brewer TF, Berkey CS, Wilson ME, Burdick E, Fineberg HV, Mosteller F. Efficacy of BCG vaccine in the prevention of tuberculosis. Meta-analysis of the published literature. JAMA 1994;271:698–702.
[4] Tameris MD, Hatherill M, Landry BS, Scriba TJ, Snowden MA, Lockhart S, Shea JE, McClain JB, Hussey GD, Hanekom WA, Mahomed H, McShane H, MVA85A 020 Trial Study Team. Safety and efficacy of MVA85A, a new tuberculosis vaccine, in infants previously vaccinated with BCG: a randomised, placebo-controlled phase 2b trial. Lancet 2013 Mar 23;381(9871):1021–8.
[5] Scanga CA, Flynn JL. Modelling tuberculosis in nonhuman primates. Cold Spring Harb Perspect Med 2014;4:a018564.
[6] Peña JC, Ho WZ. Monkey models of tuberculosis: lessons learned. Infect Immun 2015 Mar;83(3):852–62.
[7] Kaushal D, Mehra S, Didier PJ, Lackner AA. The non-human primate model of tuberculosis. J Med Primatol 2012;41:191–201.
[8] Barclay WR, Anacker RL, Brehmer W, Leif W, Ribi E. Aerosol-induced tuberculosis in subhuman primates and the course of the disease after intravenous BCG vaccination. Infect Immun 1970;2:574–82.
[9] Ribi E, Anacker RL, Barclay WR, BrehmerW Harris SC, Leif WR, Simmons J. Efficacy of mycobacterial cellwalls as a vaccine against airborne tuberculosis in the Rheus monkey. J Infect Dis 1971;123:527–38.
[10] Janicki BW, Good RC, Minden P, Affronti LF, Hymes WF. Immune responses in rhesus monkeys after bacillus Calmette–Guérin vaccination and aerosol challenge with *Mycobacterium tuberculosis*. AmRev Respir Dis 1973;107:359–66.
[11] Langermans JA, Andersen P, van Soolingen D, Vervenne RA, Frost PA, van der Laan T, van Pinxteren LA, van den Hombergh J, Kroon S, Peekel I, et al. Divergent effect of bacillus Calmette–Guérin (BCG) vaccination on *Mycobacterium tuberculosis* infection in highly related macaque species: implications for primate models in tuberculosis vaccine research. Proc Natl Acad Sci 2001;98:11497–502.
[12] Sugawara I, Sun L, Mizuno S, Taniyama T. Protective efficacy of recombinant BCG Tokyo (Ag85A) in rhesus monkeys (Macaca mulatta) infected intratracheally withH37Rv*Mycobacterium tuberculosis*. Tuberculosis 2009;89:62–7.
[13] Verreck FA, Vervenne RA, Kondova I, van Kralingen KW, Remarque EJ, Braskamp G, van der Werff NM, Kersbergen A, Ottenhoff TH, Heidt PJ, et al. MVA.85A boosting of BCG and an attenuated, phoP deficient *M. tuberculosis* vaccine both show protective efficacy against tuberculosis in rhesus macaques. PloS One 2009;4:e5264.
[14] Sharpe SA, McShane H, Dennis MJ, Basaraba RJ, Gleeson F, Hall G, McIntyre A, Gooch K, Clark S, Beveridge NE, et al. Establishment of an aerosol challenge model of tuberculosis in rhesus macaques and an evaluation of endpoints for vaccine testing. Clin Vaccine Immunol 2010;17.
[15] Rahman S, Magalhaes I, Rahman J, Ahmed RK, Sizemore DR, Scanga CA,Weichold F, Verreck F, Kondova I, Sadoff J, et al. Prime-boost vaccination with rBCG/rAd35 enhances CD8þ cytolytic T-cell responses in lesions from *Mycobacterium tuberculosis* – infected primates. Mol Med 2012;18:647–58. 1170–1182.
[16] Okada M, Kita Y, Nakajima T, Kanamaru N, Hashimoto S,Nagasawa T, Kaneda Y, Yoshida S, Nishida Y, Nakatani H, et al. Novel prophylactic and therapeutic vaccine against tuberculosis. Vaccine 2009;27:3267–70.
[17] Reed SG, Coler RN, Dalemans W, Tan EV, DeLa Cruz EC, Basaraba RJ, Orme IM, Skeiky YA, Alderson MR, Cowgill KD, et al. Defined tuberculosis vaccine, Mtb72F/AS02A, evidence of protection in cynomolgus monkeys. Proc Natl Acad Sci 2009;106:2301–6.
[18] Kita Y, Okada M, Nakajima T, Kanamaru N, Hashimoto S, Nagasawa T, Kaneda Y, Yoshida S, Nishida Y, Nakatani H, et al. Development of therapeutic and prophylactic vaccine against tuberculosis using monkey and transgenic mice models. Hum Vaccin 2011;7:108–14.
[19] Lin PL, Dietrich J, Tan E, Abalos RM, Burgos J, Bigbee C, Bigbee M, Milk L, Gideon HP, Rodgers M, et al. The multistage vaccine H56 boosts the effects of BCG to protect cynomolgus macaques against active tuberculosis and reactivation of latent *Mycobacterium tuberculosis* infection. J Clin Invest 2012;122:303–14.
[20] Sharpe SA, Eschelbach E, Basaraba RJ, Gleeson F, Hall GA, McIntyre A, Williams A, Kraft SL, Clark S, Gooch K, Hatch G, Orme IM, Marsh PD, Dennis MJ. Determination of lesion volume by MRI and stereology in a macaque model of tuberculosis. Tuberc Nov 2009;89:405–16.
[21] Lewinsohn DM, Tydeman IS, Frieder M, Grotzke JE, Lines RA, Ahmed S, Prongay KD, Primack SL, Colgin LM, Lewis AD, Lewinsohn DA. High resolution radiographic and fine immunologic definition of TB disease progression in the rhesus macaque. Microbes Infect 2006;8:2587–98.
[22] Rayner EL, Pearson GR, Hall GA, Basaraba RJ, Gleeson F, et al. Early lesions following aerosol infection of rhesus macaque (*Macaca mulatta*) with *Mycobacterium tuberculosis* strain H37Rv. J Comp Path 2013;149:475–85.
[23] Lin PL, Coleman T, Carney JP, Lopresti BJ, Tomko J, Fillmore D,Dartois V, Scanga C, Frye LJ, Janssen C, Klein E, Barry III CE, Flynn JL. Radiologic responses in cynomolgus macaques for assessing tuberculosis chemotherapy regimens. Antimicrob Agents Chemother 2013;57:4237–44.
[24] Clark S, Hall Y, Kelly D, Hatch G, Williams A. Survival of *Mycobacterium tuberculosis* during experimental aerosolisation and implications for aerosol challenge models. Appl Microbiol 2011 Aug;111(2):350–9.
[25] Druett HA. A mobile form of the Henderson apparatus. J Hyg Lond 1969;67:437–48.
[26] Hartings JM, Roy CJ. The automated bioaerosol exposure system: preclinical platform development and a respiratory dosimetry application with nonhuman primates. J Pharmacol Toxicol Methods 2004 Jan-Feb;49(1):39–55.
[27] Rayner EL, Pearson GR, Hall GA, Gleeson F, McIntyre A, Smyth D, Dennis MJ, Sharpe SA. Early lesions following aerosol challenge of rhesus macaques (Macaca mulatta) with *Mycobacterium tuberculosis* (Erdman strain). J Comp Pathol 2015 Feb-Apr;152(2–3):217–26.
[28] Dennis M, Parks S, Bell G, Taylor I, Lakeman J, Sharpe SA. A flexible approach to imaging in ABSL-3 laboratories. Appl Biosaf 2015;20(2).
[29] Sibley White L, Dennis MJ, Gooch K, Betts G, Reyes-Sandoval A, Williams A, Marsh PD, McShane H, Sharpe SA. An evaluation of the immunogenicity of MVA85A delivered by aerosol to the lungs of macaques. Clin Vaccine Immunol 2013;20(5):663–72.
[30] Lin PL, Ford CB, Coleman MT, Myers AJ, Gawande R, Ioerger T, Sacchettini J, Fortune SM, Flynn JL. Sterilization of granulomas is common in active and latent tuberculosis despite within-host variability in bacterial killing. Nat Med 2014 Jan;20(1):75–9. http://dx.doi.org/10.1038/nm.3412.
[31] Chaparas SD, Good RC, Janicki BW. Tuberculin-induced lymphocyte transformation and skin reactivity monkeys vaccinated or not vaccinated with bacille Calmette-Guerin, then challenged with virulent *Mycobacterium tuberculosis*. Am Rev Respir Dis 1975;112:43–7.
[32] Shen Y, Zhou D, Qiu L, Lai X, Simon M, Shen L, Kou Z, Wang Q, Jiang L, Estep J, Hunt R, Clagett M, Sehgal PK, Li Y, Zeng X, Morita CT, Brenner MB, Letvin NL, Chen ZW. Adaptive immune responses of Vγ2Vδ2+ T cells during mycobacterial infections. Science 2002;295:2255–8.
[33] Capuano SV, Croix DA, Pawar S, Zinovik A, Myers A, Lin PL, Bissel S, Fuhrman C, Klein E, Flynn JA. Experimental *Mycobacterium tuberculosis* infection of cynomolgus macaques closely resembles the various manifestations of human *M. tuberculosis* infection. Infect Immun 2003;71:5831–44.
[34] Gormus BJ, Blanchard JL, Alvarez XH, Didier PJ. Evidence for a rhesus monkey model of asymptomatic tuberculosis. J Med Primatol 2004;33:134–45.

[35] Lin PL, Rodgers M, Smith L, Bigbee M, Myers A, Bigbee C, Chiosea I, Capuano SV, Fuhrman C, Klein E, Flynn JL. Quantitative comparison of active and latent tuberculosis in the cynomolgus macaque model. Infect Immun 2009;77:4631–42.

[36] Lin PL, Myers A, Smith L, Bigbee C, Bigbee M, Fuhrman C, Grieser H, Chiosea I, Voitenek NN, Capuano SV, Klein E, Flynn JL. Tumor necrosis factor neutralization results in disseminated disease in acute and latent *Mycobacterium tuberculosis* infection with normal granuloma structure in a cynomolgus macaque model. Arthritis Rheum 2010;62:340–50.

[37] Green AM, Mattila JT, Bigbee CL, Bongers KS, Lin PL, Flynn JL. CD4 regulatory T cells in a cynomolgus macaque model of *Mycobacterium tuberculosis* infection. J Infect Dis 2010;202:533–41.

[38] Zhang J, Ye YQ, Wang Y, Mo PZ, Xian QY, Rao Y, Bao R, Dai M, Liu JY, Guo M, Wang X, Huang ZX, Sun LH, Tang ZJ, Ho WZ. *M. tuberculosis* H37Rv infection of Chinese rhesus macaques. J Neuroimmune Pharmacol 2011;6:362–70.

[39] MH1 Larsen, Biermann K, Chen B, Hsu T, Sambandamurthy VK, Lackner AA, Aye PP, Didier P, Huang D, Shao L, Wei H, Letvin NL, Frothingham R, Haynes BF, Chen ZW, Jacobs Jr WR. Efficacy and safety of live attenuated persistent and rapidly cleared *Mycobacterium tuberculosis* vaccine candidates in non-human primates. Vaccine 2009 Jul 23;27(34):4709–17.

[40] Roodgar M, Lackner A, Kaushal D, Sankaran S, Dandekar S, Satkoski Trask J, Drake C, Smith DG. Expression levels of 10 candidate genes in lung tissue of vaccinated and TB-infected cynomolgus macaques. J Med Primatol 2013;42:161–4.

[41] Darrah PA, Bolton DL, Lackner AA, Kaushal D, Aye PP, Mehra S, Blanchard JL, Didier PJ, Roy CJ, Rao SS, Hokey DA, Scanga CA, Sizemore DR, Sadoff JC, Roederer M, Seder RA. Aerosol vaccination with AERAS-402 elicits robust cellular immune responses in the lungs of rhesus macaques but fails to protect against high-dose *Mycobacterium tuberculosis* challenge. J Immunol 2014;193:1799–811.

[42] Flynn JL. Lessons from experimental *Mycobacterium tuberculosis* infections. Microbes Infect 2006;8:1179–88.

[43] Good RC. Simian tuberculosis: immunologic aspects. Ann N. Y Acad Sci 1968;154:200–13.